Advances in Radiation Oncology (2025) **10**, 101758

advances in radiation oncology

www.advancesradonc.org

Scientific Article

Quantification and Dosimetric Impact of Normal Organ Motion During Adaptive Radiation Therapy Planning Using a 1.5 Tesla Magnetic Resonance–Equipped Linear Accelerator (MR-Linac)

David Wittmann, MD,[a] Eric S. Paulson, PhD,[a] Anjishnu Banerjee, PhD,[a] Leou Ismael Banla, MD, PhD,[b] Christopher Schultz, MD,[a] Musaddiq Awan, MD,[a] Xinfeng Chen, PhD,[a] Eenas A. Omari, PhD,[a] Michael Straza, MD, PhD,[a] X. Allen Li, PhD,[a] Beth Erickson, MD,[a] and William A. Hall, MD[a,*]

[a]*Department of Radiation Oncology, Medical College of Wisconsin, Milwaukee, Wisconsin; and* [b]*Department of Radiation Oncology, Brigham and Women's Hospital, Boston, Massachusetts*

Received 22 May 2024; accepted 14 January 2025

Purpose: Patients receiving adaptive magnetic resonance guided radiation therapy (MRgRT) undergo contour modification prior to treatment delivery, which takes 15 to over 60 minutes. We hypothesized that during the time required to create an adaptive MRgRT plan, organ movement will result in dosimetric changes to regional organs at risk (OARs). This study quantifies the dosimetric impact of OAR motion during the time required to perform adaptive MRgRT.

Methods and Materials: Thirty-one patients with pancreatic adenocarcinoma, prostate adenocarcinoma, hepatocellular carcinoma, and oligo-metastases who received MRgRT using a 1.5 Tesla MR-Linac were prospectively enrolled in an open registry imaging trial (NCT03500081). Two magnetic resonance imaging (MRI) studies were acquired predelivery for each MRgRT treatment fraction: an initial "pretreatment" MRI (input to the adaptive evaluation with or without recontouring and replanning process), and a second "verification MRI" (acquired after the recontouring and adaption process and immediately before treatment delivery or "beam-on"). On the verification MRI, normal organs were recontoured offline. Recontoured normal organs included the colon, duodenum, small bowel, and stomach. Differences in OARs between organ positions represented the normal organ movement during the time required for plan adaption. Maximum dose (Dmax), volumetric (V) 0.5 cubic centimeter dose (D0.5cc), 3000 cGy (V30), and 2000 cGy (V20) were calculated from the recontoured verification MRI.

Results: Differences in Dmax, per fraction, for the listed normal organs were as follows: colon/rectum 239.50 cGy ($P = .09$), duodenum 136.40 cGy ($P = .05$), small bowel 488.27 cGy ($P < .01$), and stomach 95.92 ($P = .17$). Small bowel demonstrated a significant difference in Dmax, D0.5cc, and V30.

Conclusions: Statistically significant differences in small bowel doses are demonstrated as a result of motion during the timing required for adaptive MRgRT. These results reflect the importance of verifying MRI acquisition during adaptive MRgRT to confirm the location of OARs. They also identify the necessity of strategies to account for the dynamic nature of regional OARs.

Sources of support: There was no funding for this work.

Research data are stored in an institutional repository and will be shared on request to the corresponding author.

*Corresponding author: William A. Hall, MD; Emails: eomari@mcw.edu whall@mcw.edu

https://doi.org/10.1016/j.adro.2025.101758

Introduction

Radiation therapy (RT) is a highly effective treatment option for many cancers. Adaptive magnetic resonance guided radiation therapy (MRgRT) is a recent and novel method of delivering RT[1-5] with the unique advantage of real-time ("online") imaging during the treatment process.[6] With this technology, tumor position and local organs at risk (OARs) can be accounted for in real-time. MRgRT enables correction for normal organ positional variation that is observed during daily treatment.

Adaptive RT requires an initial plan generation using a simulation image (typically a CT scan) which generates a reference plan outlining the position of treatment targets as well as local OARs. This initial reference plan serves as a starting point for the treatment planning process. Before each daily treatment, the initial reference plan is subsequently adapted with the patient on the treatment table. The adaptive plan accounts for the movement of normal organs that occurs between the initial reference plan generation and the daily adaptive fraction delivery.[2]

The process of daily adaption takes considerable time. Although adaption of the plan is ongoing, the patient is on the treatment table for a duration of 15 minutes to over 60 minutes.[6] During the time required for adaption, it has been consistently observed that local organs in the region of the tumor exhibit some movement. Such movement is especially true for organs within the abdomen and pelvis and is likely due to physiological processes such as breathing and peristalsis. It also appears that the magnitude of this movement differs depending on the specific organ. For example, we have observed in patients at our institution that the colon and stomach appear to move differently than the small bowel. Normal organ movement due to these physiological processes during adaption may impact delivered radiation doses to these organs. Specifically, this phenomenon can, and likely does, result in these organs moving either into or away from a higher dose region of RT during the time required for adaption. We, therefore, hypothesize that normal organ movement during the time required to create an adapted RT plan results in unanticipated doses delivered to local OARs.

In this study, we investigate a range of abdominal OARs and how motion during plan adaption potentially impacts the radiation dose delivered to these organs. Specifically, we quantified the dosimetric impact of normal organ motion during the time required to perform adaptive MRgRT. Furthermore, we sought to understand the necessity of a verification magnetic resonance imaging (MRI) acquisition immediately before beam-on. Our institutional practice has been to acquire a verification MRI immediately before beam-on to assess normal organ position and estimate treatment plan safety prior to delivery. However, prior to this study, it remained unknown whether normal organ movement during the time required for adaption nullifies this entire process. In other words, the question arises of whether the organs move so much during adaption that the actual adapted contours are no longer relevant (or even necessary).

Methods and Materials

Protocol and device

Patients were recruited if they underwent treatment on the 1.5 Tesla MR-Linac at Froedtert and the Medical College of Wisconsin from January 2019 to June 2021. All patients were treated on a 1.5-Tesla magnetic resonance (MR) equipped linear accelerator (MR-Linac, Unity, Elekta AB) for MRgRT.

Each patient consented to enrollment in an institutional-based institutional review board–approved prospective observation study (NCT03500081). Patients provided written informed consent for clinical and technical data to be obtained, along with additional quantitative and 4D MR images to be acquired during treatment with RT. This study was approved by the Medical College of Wisconsin.

Simulation imaging and treatment planning

Each patient underwent standard CT simulation. A reference plan was created based on the simulation CT and often registered with an MR simulation. Motion management was accomplished using an internal target volume approach, which was created based on the free-breathing 4D CT simulation. Planning target volume margins ranged from approximately 0.3 to 0.5 cm. In addition, a 4D MRI was used to confirm adequate coverage of moving targets. Reference plans for treatment on the MR-Linac and backup plans for treatment on a conventional Linac system that used CT-based image guidance were created using Monaco treatment planning software (Elekta AB).

Day of treatment procedures and intratreatment imaging

Our institutional workflows and imaging protocols have been previously published; this study in particular pertains to our adapt-to-shape (ATS) workflow.[7] In brief, a treatment checklist was designed for use during daily treatment and was used before and during each treatment procedure. Prebeam T1 or mixed T2/T1-weighted 4D MRIs were acquired. Motion-averaged or midposition images were reconstructed using a separate high-performance reconstruction server positioned within the MR-Linac network. Quantitative intravoxel incoherent motion diffusion-weighted imaging and T2 mapping were

acquired concurrently during plan adaption with ATS workflows.[6] An ATS workflow involves recontouring all normal organs and confirming the tumor contour on a daily basis. An ATS is performed to account for all interfraction changes by reoptimizing the plan based on the MRI acquired on the day of treatment with a fully updated contour set. This treatment strategy has also been previously described.[8] Real-time cine 2D MRIs acquired in 3 perpendicular planes through the planning target volume center of mass were used to monitor the target during radiation delivery. A verification image is acquired immediately before the beam-on. Per our institutional standard of practice, treatment was administered if the plan was conformal, contours were adapted if only small adjustments were needed to meet conformality requirements after which treatment was delivered, or treatment was aborted if there were too large discrepancies in organ position between the planning scan and verification image. Such treatment decisions were at the discretion of the attending radiation oncologist.

Data collection and analysis

MRIs acquired from the aforementioned prospective observational study and an open registry trial (MOMENTUM, NCT04075305) were collected in MIM (MIM Software Inc). MIM is an imaging analysis software that enables detailed image visualization, collation, and computing of dose distribution. On the day of treatment per ATS workflow, the patient underwent 2 different sets of MRI scans. The first MRI (called "preadaption MRI" going forward) was used to confirm regional anatomy. Adjustments to the plan were made accordingly based on changes to the regional anatomy. A second scan (called "verification MRI" going forward) was obtained immediately prior to beam-on to account for any normal organ movement during adaption. Differences in normal organ position between these 2 MRI scans represented the normal organ movement during the time required for treatment adaption and verification. The verification image is a 3D image that enables adjustment of the daily adaptive plan for baseline drifts occurring between the acquisition of the prebeam image (ie preadaption MRI) and the start of treatment. These baseline drifts can be caused by patient relaxation, patient sinking into the padding on the couch or internal motion. Real-time 2D cine images can be used to pause the beam during delivery but cannot be used to correct the adaptive plan for the baseline drift prior to the start of delivery. Schematically this is represented in Fig. 1.

To calculate the dosimetric impact of organ motion, the normal organs near the radiation targets were retrospectively contoured on the verification MRI for each fraction of every enrolled patient. Regardless of the primary tumor site, all contoured normal OARs for each treatment fraction for each patient included stomach, duodenum, colon, and small bowel. Dosimetric values

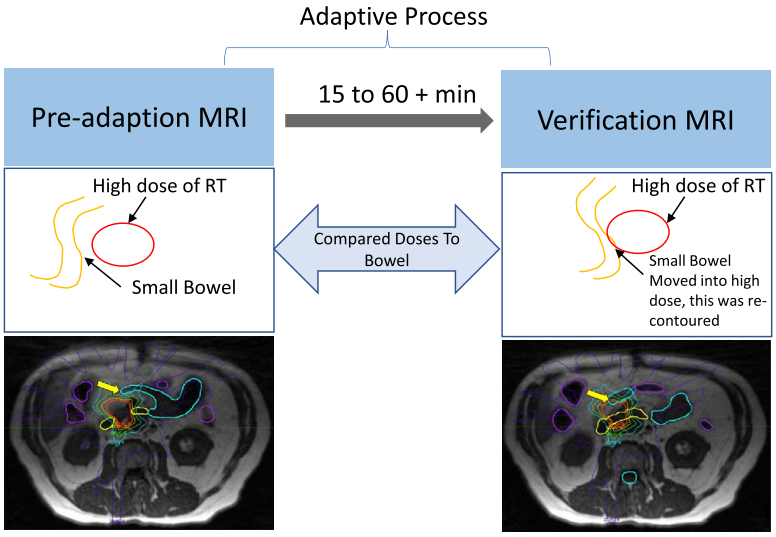

Figure 1 Treatment course on the MR-Linac. An initial magnetic resonance imaging (MRI) is obtained (preadaption MRI) to compare the original planning CT scan with the patient's internal anatomy on the day of treatment. Adjustments are made over a period of 15 to over 60 minutes using the preadaption MRI. Once completed, a second "verification" image (verification MRI) is obtained immediately before beam-on to ensure there were no major shifts in internal anatomy during the dose adjustment period. A real patient example is shown below the illustration: preadaption MRI (left) is used to adjust the treatment plan for the anatomy of the day. Verification MRI (right) is used to document normal organ motion during the time required for adaptive radiation therapy (RT) plan generation. This figure demonstrates the dose distribution noted by the concentric rings, as well as duodenum in bright yellow, colon in purple, and small bowel in teal. Note the small bowel and duodenum migration (yellow arrow) into an area of high dose distribution during the time required for plan adaption.

derived from the verification MRI contours for each treatment fraction were subsequently compared to the contours and dose distribution generated on the day of treatment on the preadaption MRI via extraction of maximum dose (Dmax), dose at 0.5 cc (D0.5cc), volume receiving 2000 cGy (V20), and volume receiving 3000 cGy (V30) from dose-volume histogram spreadsheets generated in MIM for both the preadaption MRI and the verification MRI. Data analysis for the aforementioned parameters consisted of mean and absolute differences in dosage and volumes between the 2 MRI scans, summary statistics versus the mean value, Bland-Altman plots, and a mixed-effects linear model with fixed and random effects. Statistical analyses were performed using SAS 9.4 (SAS Institute).

Results

Patient characteristics

A total of 31 ATS patients were included. Median age was 68 years (range, 47-90). Treated tumor types included adrenal cancer, endometrial cancer metastasis, gastric cancer, hepatocellular carcinoma, intrahepatic cholangiocarcinoma, liver metastases, metastatic renal cell carcinoma, pancreatic adenocarcinoma, prostatic adenocarcinoma, and sarcoma. The median dose was 3500 cGy (range, 2400-6000 cGy) delivered over 3 to 5 fractions. Full patient characteristics, tumor types treated, and prescription doses are reported in Table 1.

Table 1 Clinical characteristics of study participants

Variables	All patients N = 31 (%)
Age (y)	
Median (min-max)	68 (47-90)
Mean ± SD	69 ± 10
Sex	
Female	11 (36)
Male	20 (64)
Tumor type	
Metastatic cancer of the adrenal gland	3 (10)
Metastatic endometrial cancer	2 (6)
Metastatic gastric cancer	1 (3)
Hepatocellular carcinoma	4 (13)
Intrahepatic cholangiocarcinoma	1 (3)
Metastatic lung cancer to liver	1 (3)
Metastatic melanoma to liver	1 (3)
Metastatic renal cell carcinoma	3 (10)
Pancreatic adenocarcinoma	10 (32)
Prostatic adenocarcinoma	4 (13)
Metastatic Sarcoma	1 (3)
Total dose (cGy)	
Median (min-max) over 3-5 fractions	3500 (2400-6000)
Mean ± SD	3751 ± 854
BMI (kg/m^2)	
Median (min-max)	27 (18-37)
Mean ± SD	27 ± 5

Abbreviations: BMI = body mass index.

Treatment timing and dosimetric measurements

The median time between the acquisition of the preadaption MRI and the verification MRI was 36 minutes (range, 7-98 minutes). Contours of normal organs including the colon, duodenum, small bowel, and stomach were manually segmented on the verification MRIs. Most of the regional organs did not demonstrate a statistically significant difference in doses. Small bowel, however, demonstrated a statistically significant (higher) difference in Dmax, D0.5cc, V20, and V30. Differences specifically in Dmax doses are demonstrated in Table 2. Similarly, differences for D0.5cc, V20, and V30 are listed in Table E1.

A plot comparing the preadaption MRI and the verification MRI dose distributions for local OARs is shown in Fig. 2. Each axis on this figure represents radiation dose Dmax calculated before adaption (x-axis) and then after adaption (y-axis) on the verification MRI. There are many notable instances that fall into ranges of dosimetry change that are highly clinically significant. For instance, some small bowel treatment fractions incurred a 20 Gy increase in max dose between the acquisition of the preadaption MRI and the verification MRI. Note the significantly higher postadaption doses in the small bowel relative to other organs which exhibited minimal change between the acquisition of the preadaption MRI and the verification MRI. A particularly interesting example is shown at the bottom of Fig. 1. The relative mean dose differences and absolute mean dose differences of the normal organs between the preadaption MRI and the verification MRI are summarized in Table E2.

Discussion

We have presented the first study, to our knowledge, to comprehensively characterize the magnitude and dosimetric impact of normal organ movement during the time required for plan adaption using a 1.5 Tesla MR-Linac. These data reveal that in some organs, particularly

Table 2 Difference in Dmax per fraction between preadaption MRI and verification MRI for the listed contoured organs at risk

Organ	Difference (cGy)	*P* value	Lower CI (cGy)	Upper CI (cGy)
Colon	239.50	.0957	−43.0154	522.02
Duodenum	136.40	.0519	−1.1476	273.95
Small bowel	488.27	.0008	208.45	768.08
Stomach	95.9239	0.1745	−43.2409	235.09

Abbreviations: Dmax = maximum dose; MRI = magnetic resonance imaging.

the small bowel, the time required for daily adaption can result in marked dosimetric differences. As reflected by the data presented, these differences can be rather dramatic. Without the acquisition of a verification MRI immediately before beam-on, these data would not have been known or understood. Such differences highlight the importance of a verification MRI acquisition immediately pretreatment, along with continuous imaging during beam delivery.

Adaptive RT executed using MR guidance is rapidly expanding within the specialty of radiation oncology, but novel aspects of this process require comprehensive evaluation.[9] Daily MRgRT adaption is becoming more feasible with the commercial introduction of MR-equipped linear accelerators. Although adaption in the upper abdomen is highly appealing and offers the advantage of improved soft tissue visualization, it is also time-consuming. Specifically, this often takes over 30 minutes including the process of recontouring and plan creation, even at experienced centers.[6] This calls into question the clinical utility and feasibility of current approaches to daily adaptive MRgRT. Our study reflects the importance of a verification image acquisition during this process, and although time-consuming, this critical step necessitates an evaluation

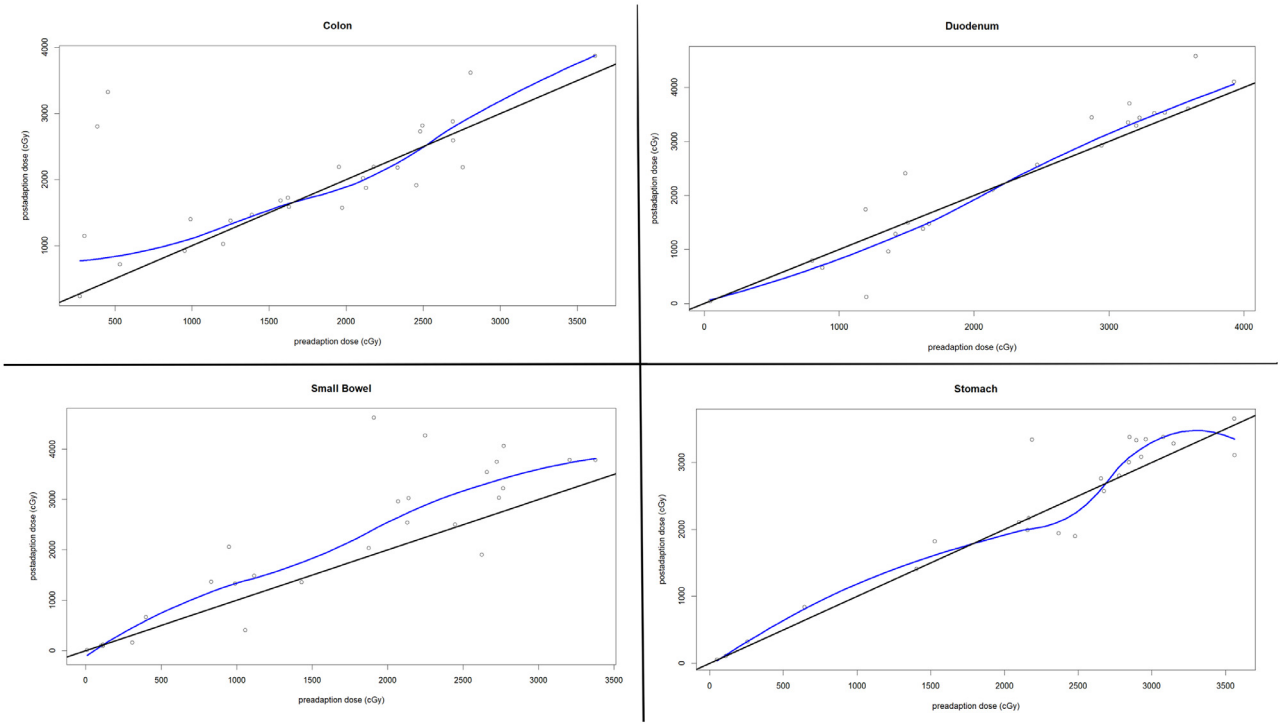

Figure 2 Plot comparing the preadaption magnetic resonance imaging (MRI) (x-axis) and the verification MRI (y-axis, labeled as "postadaption" on the graph) Dmax dose distribution for various local organs at risk (OARs). Note that each dot represents a single average for each patient's complement of contours for the listed OARs. A trajectory along the black midline indicates similarity between preadaption MRI and verification MRI dose distribution to critical local OARs. The blue lines represent locally weighted scatterplot smoothing generated via robust locally weighted regression. That is to say, in contrast to a simple linear model which fits a straight line through a set of points, a locally weighted scatterplot smoothing model fits a curved line through the same set of points. This can be thought of as a "moving average" or the best possible curved fit through a set of points. This is best used when analyzing nonlinear relationships as more weight can be given to data points that are more conformal to the variables being analyzed with less weight given to outliers. Note the presence of significant outliers, tending toward higher postadaptive small bowel doses relative to other studied organs which exhibited minimal change during plan adaption.

of normal organ motion and its associated dosimetric impact.

Critical and implicit in our findings is the concept that radiation is a dynamic process that requires constant oversight. Incorporation of a time component into dose-volume histogram data could even be a direct avenue for future research development. The idea that RT dose is modeled with a static scan (CT or MRI) representative of a single time point is quickly becoming archaic. Normal organs are constantly moving and MRgRT has enabled radiation oncologists to visualize such movement. Strategies to understand and account for the dosimetric impact of this movement should be the focus of future research. Until radiation oncologists can clearly account for accumulated doses to normal organs during each fraction and over the course of treatment, models based on movement seen on a verification MRI are an essential use of existing technology to account for this.

Several existing publications have characterized the dosimetric and volumetric changes to local OARs for various cancer types.[6,8-19] One study by Gandhi et al[20] used SmartAdapt deformable image registration to estimate volume changes and dose differences in local OARs for prostate cancer. Another study investigated the effect of intratreatment bladder and rectum volume changes on cumulative dose to these organs in patients treated for prostate cancer.[21] Although these studies provide important insights into dose discrepancies based on volumetric changes, they are somewhat limited in scope compared to our presented data because the only OARs evaluated were the rectum and bladder. Our study provides some novelty in that we have comprehensively characterized the dosimetric impact of normal organ motion encountered during adaptive MRgRT for a variety of abdominopelvic tumors and their various associated OARs.

Studies involving MR-equipped linear accelerators have resulted in new ways of understanding and visualizing the OAR movement that occurs during the time required for RT plan adaption. Some of these recent studies have also indicated that interfraction organ movement may result in significant dose differences between planned and delivered doses to local OARs.[22-29] One study by Palacios et al[22] noted significant interfractional changes in OARs (stomach, bowel, duodenum) position and underdosage of target volumes during plan recalculation based on the anatomy of the day, which resulted in failure to meet institutional constraints in one-third of patients. Online target reoptimization improved target coverage in nearly two-thirds of fractions.[22] In another study, patients with pancreatic or liver cancers treated via MRgRT were found to have peristalsis-induced OAR motion ranging from 0.3 to 1.0 cm. This study further characterized the degree of motion due to respiratory motions in addition to peristalsis. However, in comparison to the findings we have presented above, this study differed in that the center of mass motion was used for the motion assessment, and does not well characterize the motion of organs experiencing large deformations such as the small bowel which was excluded.[24] This is an important difference compared to our study above as the small bowel was found to exhibit motion characteristics resulting in statistically significant dosimetric differences incurred during the adaptive MRgRT process. It remains to be determined whether the differences found are clinically significant. However, the observed changes are in dose ranges that would be considered to be clinically significant fluctuations.[30-32]

Statistically significant differences in small bowel doses are demonstrated when doses are calculated using the verification MRI. This is likely due to the small bowel's inherent mobility compared to the other organs analyzed. No other abdominal organ dose differences between scans proved statistically significant; however, unique outlier circumstances can be clearly seen in Fig. 2. We feel that these data reflect the importance of pretreatment verification MRIs during adaptive stereotactic RT for all abdominal tumors, despite the absence of significance for other normal OARs. There may be less of an impact on some organ locations; however, clearly the presence of outliers is ubiquitous across several different OARs.

There are limitations to this analysis that warrant discussion. First, our sample size was limited to 31 patients. This limitation was somewhat pragmatic given the timing of the project which embarked shortly after our institution opened the MR-Linac for treatment and had an adequate number of patients enrolled in our prospective open registry trials. We were one of the original institutions in the United States to acquire the 1.5 Tesla MR-Linac unit, and this study's participants were some of the first patients enrolled for treatment. Additionally, our sample size was a result of the time commitment required to recontour each verification image for each treatment fraction for each patient, which amounted to more than 100 new individually recontoured scans. Considering more than 5 organs per scan, this is well over 500 individually recontoured organs. As such, given the timing of the work performed and the dedicated availability of the individual performing the work, the project was limited to 31 patients. A larger sample size would have improved the statistical power of the study. Future projects can certainly expand on these data further, and increasing commercial availability of MR-equipped linear accelerators would enable larger similar analyses which would certainly improve the generalizability of the data. Artificial intelligence—assisted contouring may add efficacy to this process. When considering other limitations, it is important to take into account the influence of patient preparation and setup on the frequency and/or magnitude of organ motion during the treatment time. Given that each patient served as his/her own control in the sense that organ positions were recontoured and compared to that same patient's original scans, differences in setup should be less

impactful as a result. These normal organ positions were clearly visualized and confirmed by an experienced radiation oncologist, thus mitigating the effects of interobserver variability. Another limitation was the fact that we have not included the impact of these verification MRIs on mitigation of patient toxicity. This was a clear decision, because our institutional practice was to either terminate treatment or perform an additional adaption if there was considerable movement of critical local normal organs. Such interventions based on the findings of the verification MRI scans likely mitigated the potential toxicity associated with these variations. An additional limitation for consideration is that the dosimetric impact was based on recontouring and subsequent dose reconstruction without the reoptimization based on the updated anatomy on verification MRI. This was anticipated to have only resulted in minimal total differences in dose. Given the magnitude of dosimetric changes seen (in some cases greater than 20 Gy), it is unlikely this would have been substantially impacted by plan reoptimization, but this possibility is important to consider. Lastly, our study included patients with various primary tumor sites. The location of the primary tumor that was treated was not accounted for and could have impacted the measured doses to regional OARs.

Intrafraction organ motion monitoring is equally critical to measuring organ motion during plan adaption. Although limited in number, studies investigating such intrafraction organ motion do exist and attempt to better characterize the associated dosimetric impact of organ motion due to factors outlined previously, including breathing motion and peristalsis. In our study, patients did not have any specific bowel preparation such as an antiperistaltic agent, and compression was not routinely used in this time period. A future direction may consider comparing these results to those of patients managed with compression or bowel motion management. Regarding respiratory motions, one example by Ali Mirzapour et al[33] developed both semi-Markov and Markov models to predict organ motion between phases of a respiratory cycle along with transitions to future respiratory cycles. The intended application of this exciting work is for online organ tracking and therapy reoptimization.[33] Although our study focused on quantifying the dosimetric impact of organ motion during adaption, a future direction could be directly modeling anticipated movement and predicting clinical circumstances in which such movement would occur. Such work is underway. Lastly, the results of this study reflect our institutional experience regarding the dosimetric impact of organ motion during the time required for adaptive MRgRT. The enrolled patients were some of the first in the country to be treated on an MR-equipped linear accelerator. Since this time, the commercial availability of such machines has rapidly increased, and various institutions are now much more experienced with plan adaption and motion management. Thus, extrapolation of our single institution data on a wider scale would certainly improve this study's generalizability as the specialty of radiation oncology continues to increasingly embrace the capabilities of adaption-based treatment. Management of these data continues to evolve with the art of radiation delivery. A visual review of this overlay by the attending radiation oncologist is needed. Critical in this process is the clinical judgment of the patient, medical comorbidities, and specific malignancy being treated.

In conclusion, this study suggests verification image acquisition, immediately prior to beam-on, is important to ensure that the result of MR guidance-based plan adaption remains accurate at the time of dose delivery. More specifically, a verification image acquired immediately before beam-on is important to ensure the position of normal organs that may have changed significantly during plan adaption. Future short-term research should focus on methods to shorten the adaption duration to minimize the time for unfavorable organ migration. Longer-term research will need to focus on the concept of "dynamic dose volume histogram modeling," in other words, real-time plan adaption could be coupled with methods that enable constant dose monitoring of moving OARs. These data illustrate "real-time temporal feathering" that has been taking place for decades of RT delivery. Understanding and accounting for this movement may dramatically improve the safety and capabilities of adaptive RT.

Disclosures

David Wittmann has nothing to disclose. Eric Paulson discloses research and travel support from Elekta AB and reports being co-founder of Sonoptima. Anjishnu Banerjee has nothing to disclose. Ismael Banla has nothing to disclose. Chris Schultz discloses travel support from Elekta AB for the MR-Linac Consortium Meeting, MR-Linac Leadership Position, and institutional research support, all outside the scope of this work. Musaddiq Awan has nothing to disclose. Xinfeng Chen has nothing to disclose. Eenas Omari discloses research and travel support from Elekta AB, outside of the scope of this work. Michael Straza has nothing to disclose. X. Allen Li discloses an institutional grant from Elekta AB, an institutional grant from Siemens, and travel support from Elekta AB, all outside the scope of this work. Beth Erickson has nothing to disclose. William A. Hall discloses consulting fees from Aktis Oncology, outside the scope of this work. William A. Hall reports being co-founder of Sonoptima, and departmental research and travel support from Elekta AB.

Acknowledgments

The authors acknowledge the patients and their families. Anjishnu Banerjee performed the statistical analysis.

Supplementary materials

Supplementary material associated with this article can be found in the online version at doi:10.1016/j.adro.2025.101758.

References

1. Hall WA, Paulson ES, van der Heide UA, et al. The transformation of radiation oncology using real-time magnetic resonance guidance: A review. *Eur J Cancer*. 2019;122:42-52.
2. Hall WA, Paulson E, Li XA, et al. Magnetic resonance linear accelerator technology and adaptive radiation therapy: An overview for clinicians. *CA Cancer J Clin*. 2022;72:34-56. https://doi.org/10.3322/caac.21707.
3. Randall JW, Rammohan N, Das IJ, Yadav P. Towards accurate and precise image-guided radiotherapy: Clinical applications of the MR-Linac. *J Clin Med*. 2022;11:4044.
4. Kurz C, Buizza G, Landry G, et al. Medical physics challenges in clinical MR-guided radiotherapy. *Radiat Oncol*. 2020;15:93.
5. Nierer L, Eze C, da Silva, Mendes V, et al. Dosimetric benefit of MR-guided online adaptive radiotherapy in different tumor entities: Liver, lung, abdominal lymph nodes, pancreas and prostate. *Radiat Oncol*. 2022;17:53.
6. Hall WA, Straza MW, Chen X, et al. Initial clinical experience of stereotactic body radiation therapy (SBRT) for liver metastases, primary liver malignancy, and pancreatic cancer with 4D-MRI based online adaptation and real-time MRI monitoring using a 1.5 Tesla MR-Linac. *PLOS One*. 2020;15:e0236570.
7. Paulson ES, Ahunbay E, Chen X, et al. 4D-MRI driven MR-guided online adaptive radiotherapy for abdominal stereotactic body radiation therapy on a high field MR-Linac: Implementation and initial clinical experience. *Clin Transl Radiat Oncol*. 2020;23:72-79.
8. Winkel D, Bol GH, Kroon PS, et al. Adaptive radiotherapy: The Elekta Unity MR-linac concept. *Clin Transl Radiat Oncol*. 2019;18:54-59.
9. Glide-Hurst CK, Lee P, Yock AD, et al. Adaptive radiation therapy (ART) strategies and technical considerations: A state of the art review from NRG oncology. *Int J Radiat Oncol Biol Phys*. 2021;109:1054-1075.
10. Schaule J, Chamberlain M, Wilke L, et al. Intrafractional stability of MR-guided online adaptive SBRT for prostate cancer. *Radiat Oncol*. 2021;16:189.
11. Padgett KR, Simpson G, Asher D, Portelance L, Bossart E, Dogan N. Assessment of online adaptive MR-guided stereotactic body radiotherapy of liver cancers. *Phys Med*. 2020;77:54-63.
12. El-Bared N, Portelance L, Spieler BO, et al. Dosimetric benefits and practical pitfalls of daily online adaptive MRI-guided stereotactic radiation therapy for pancreatic cancer. *Pract Radiat Oncol*. 2019;9:e46-e54.
13. Mayinger M, Ludwig R, Christ SM, et al. Benefit of replanning in MR-guided online adaptive radiation therapy in the treatment of liver metastasis. *Radiat Oncol*. 2021;16:84.
14. Weykamp F, Katsigiannopulos E, Piskorski L, et al. Dosimetric benefit of adaptive magnetic resonance-guided stereotactic body radiotherapy of liver metastases. *Cancers (Basel)*. 2022;14:6041.
15. Placidi L, Romano A, Chiloiro G, et al. On-line adaptive MR guided radiotherapy for locally advanced pancreatic cancer: Clinical and dosimetric considerations. *Tech Innov Patient Support Radiat Oncol*. 2020;15:15-21.
16. Dang J, Kong V, Li W, et al. Impact of intrafraction changes in delivered dose of the day for prostate cancer patients treated with stereotactic body radiotherapy via MR-Linac. *Tech Innov Patient Support Radiat Oncol*. 2022;23:41-46.
17. Willigenburg T, Zachiu C, Bol GH, et al. Clinical application of a sub-fractionation workflow for intrafraction re-planning during prostate radiotherapy treatment on a 1.5 Tesla MR-Linac: A practical method to mitigate intrafraction motion. *Radiother Oncol*. 2022;176:25-30.
18. Ruggieri R, Rigo M, Naccarato S, et al. Adaptive SBRT by 1.5 T MR-linac for prostate cancer: On the accuracy of dose delivery in view of the prolonged session time. *Phys Med*. 2020;80:34-41.
19. Brennan VS, Burleson S, Kostrzewa C, et al. SBRT focal dose intensification using an MR-Linac adaptive planning for intermediate-risk prostate cancer: An analysis of the dosimetric impact of intra-fractional organ changes. *Radiother Oncol*. 2023;179:109441.
20. Gandhi A, Vellaiyan S, Subramanian S, Swamy ST, Subramanian K, Ayyalusamy A. Application of aSi-kVCBCT for volume assessment and dose estimation: An offline adaptive study for prostate radiotherapy. *Asian Pac J Cancer Prev*. 2019;20:229-234.
21. Pearson D, Gill SK, Campbell N, Reddy K. Dosimetric and volumetric changes in the rectum and bladder in patients receiving CBCT-guided prostate IMRT: Analysis based on daily CBCT dose calculation. *J Appl Clin Med Phys*. 2016;17:107-117.
22. Palacios MA, Bohoudi O, Bruynzeel AME, et al. Role of daily plan adaptation in MR-guided stereotactic ablative radiation therapy for adrenal metastases. *Int J Radiat Oncol Biol Phys*. 2018;102:426-433.
23. Wysocka B, Kassam Z, Lockwood G, et al. Interfraction and respiratory organ motion during conformal radiotherapy in gastric cancer. *Int J Radiat Oncol Biol Phys*. 2010;77:53-59.
24. Mostafaei F, Tai A, Omari E, et al. Variations of MRI-assessed peristaltic motions during radiation therapy. *PLOS One*. 2018;13:e0205917.
25. Finazzi T, Palacios MA, Spoelstra FOB, et al. Role of on-table plan adaptation in MR-guided ablative radiation therapy for central lung tumors. *Int J Radiat Oncol Biol Phys*. 2019;104:933-941.
26. Henke LE, Kashani R, Hilliard J, et al. In silico trial of MR-guided midtreatment adaptive planning for hypofractionated stereotactic radiation therapy in centrally located thoracic tumors. *Int J Radiat Oncol Biol Phys*. 2018;102:987-995.
27. Knybel L, Cvek J, Otahal B, et al. The analysis of respiration-induced pancreatic tumor motion based on reference measurement. *Radiat Oncol*. 2014;9:192.
28. van Kranen S, Hamming-Vrieze O, Wolf A, Damen E, van Herk M, Sonke JJ. Head and neck margin reduction with adaptive radiation therapy: Robustness of treatment plans against anatomy changes. *Int J Radiat Oncol Biol Phys*. 2016;96:653-660.
29. Olberg S, Green O, Cai B, et al. Optimization of treatment planning workflow and tumor coverage during daily adaptive magnetic resonance image guided radiation therapy (MR-IGRT) of pancreatic cancer. *Radiat Oncol*. 2018;13:51.
30. Oar A, Lee M, Le H, et al. Australasian Gastrointestinal Trials Group (AGITG) and Trans-Tasman Radiation Oncology Group (TROG) guidelines for pancreatic stereotactic body radiation therapy (SBRT). *Pract Radiat Oncol*. 2020;10:e136-e146.
31. Guckenberger M, Baus WW, Blanck O, et al. Definition and quality requirements for stereotactic radiotherapy: Consensus statement from the DEGRO/DGMP Working Group Stereotactic Radiotherapy and Radiosurgery. *Strahlenther Onkol*. 2020;196:417-420.
32. Bolton VN, Braude PR, Ockenden K, Marsh SK, Robertson G, Ross LD. An evaluation of semen analysis and in-vitro tests of sperm function in the prediction of the outcome of intrauterine AIH. *Hum Reprod*. 1989;4:674-679.
33. Ali Mirzapour S, Mazur T, Sharp G, Salari E. Intra-fraction motion prediction in MRI-guided radiation therapy using Markov processes. *Phys Med Biol*. 2019;64:195006.